

Growth and Morphology Change of Polystyrene-*block*-poly(2-cinnamoyl ethyl methacrylate) Particles in Solvent–Nonsolvent Mixtures before Precipitation

Jianfu Ding and Guojun Liu*

Department of Chemistry, University of Calgary, 2500 University Dr., NW, Calgary, Alberta, Canada T2N 1N4

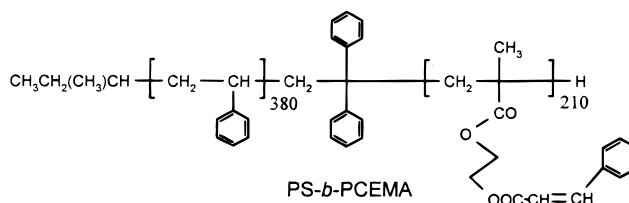
Received April 30, 1999; Revised Manuscript Received October 13, 1999

ABSTRACT: Tetrahydrofuran (THF) and acetonitrile (AN) are good and poor solvents for poly(2-cinnamoyl ethyl methacrylate) (PCEMA) and polystyrene (PS). Their mixtures with AN volume fractions between 80% and 93% are precipitants for PS but slightly solubilize the PCEMA block of a polystyrene-*block*-poly(2-cinnamoyl ethyl methacrylate), PS-*b*-PCEMA, sample with 380 styrene and 210 CEMA units. Immediately after the addition of AN to a THF solution of the diblock, spherical particles with PCEMA shell and PS core are formed due to phase separation. The core–shell particles then grow in size, presumably mainly due to particle coalescence, and transform into the more complex egglike, onionlike, and berrylike particles in THF/AN with 80%–90% AN before precipitation in several weeks. In THF/AN with 93% AN, no structural mutation is seen in 1 week after the formation of the spherical particles despite eventual polymer precipitation. This resistance of the spherical core–shell particles to morphological transitions may be due to the locking in of the PS core in a glassy state.

I. Introduction

A polymer solution undergoes phase separation if the solvation power of the medium degrades sufficiently. Of the two phases, one is rich in polymer and the other in solvent. Polymer phase separation occurs via either the spinodal decomposition or the nucleation and growth mechanism.^{1,2} Phase separation via spinodal decomposition is typically fast where both phases approach their equilibrium concentrations “simultaneously” and occurs due to the sudden and drastic worsening of the solvation medium. Phase separation takes place by nucleation and growth if the solvent is only slightly worse than Θ condition or the system is in the metastable region. Such phase separations are slow and characterized by particle nucleation, growth, and coarsening stages. During such phase separation, one phase always has equilibrium concentration, and the other phase may be supersaturated or “undercooled” initially. Polymer precipitation occurs after the phase-segregated polymer particles or microdomains coarsen into macroscopic particles and settle. Traditionally, solution phase separation studies have been concerned with homopolymers. When nucleation and growth are invoked, the growth of the particles can be followed using optical microscopy.^{3–6} The sudden immersion of a concentrated polymer film into a nonsolvent and the subsequent polymer phase separation by spinodal decomposition have served as the basis for the production of many membranes.⁷

My group has been interested in morphologies^{8–10} of diblock copolymer micelles formed in block-selective solvents or solvents that solubilize one but not the other block of a diblock copolymer. This normally involves dissolving a diblock copolymer in a mutual solvent for both blocks and then adding a block-selective solvent to induce micelle formation. When studying the micelle morphologies of polystyrene-*block*-poly(2-cinnamoyl ethyl methacrylate) or PS-*b*-PCEMA, we accidentally added a precipitant, acetonitrile (AN), for both PS and PCEMA, instead of a block-selective solvent into a THF



solution of this diblock. We observed the eventual precipitation of the polymer in several weeks. The more interesting aspects have been in the observations made before the polymer precipitated. Immediately after the addition of AN to the AN volume fractions between 80% and 93%, dense spherical PS-*b*-PCEMA particles with PS core and PCEMA shell, resembling spherical micelles structurally, were formed. The particles then grew and coarsened in THF/AN with AN between 80% and 90% probably via the fusion of different particles into the more complex egglike, onionlike, and berrylike particles. In THF/AN with 93% AN, no structural mutation is seen in 1 week after the formation of the spherical particles.

Reported in this paper is the structural clarification of the intermediate particles formed before their precipitation. This study is important because it represents the first report of diblock particle morphological evolution before precipitation. It is important also because the variously shaped intermediates should be very useful as precursors to novel polymeric nanostructures.¹¹

II. Experimental Section

Sample Preparation. A polymer with 380 styrene and 210 CEMA units was used in this study. The precursor to PS-*b*-PCEMA was synthesized by anionic polymerization as described previously.^{12,13} The sample was characterized by GPC, NMR, and light scattering, and the characterization results of the polymer are shown in Table 1.

For precipitation studies, THF and AN were dried overnight over molecular sieves. PS-*b*-PCEMA was dissolved in THF. AN was then added to the AN volume fractions of 80%–93%. In

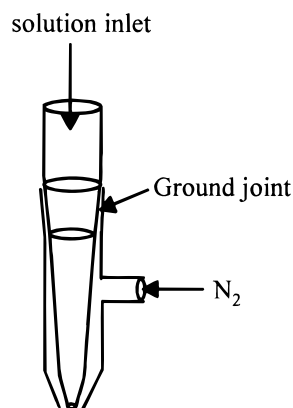


Figure 1. Apparatus for spraying solutions.

Table 1. Characteristics of the PS-*b*-PCEMA Sample Used

n/m by NMR	\bar{M}_w/\bar{M}_n by GPC	$10^{-4}\bar{M}_w$ by LS	$10^{-2}n$	$10^{-2}m$
1.8	1.08	9.4	3.8	2.1

all experiments, the final polymer concentration was at ~ 1.0 mg/mL. Particle cross-linking was achieved by irradiating well-stirred samples, 100 mL, with light that had passed a 260 nm cutoff filter from a 500 W mercury lamp.¹⁴ At various times, 2.0 mL was taken from the irradiated solution. Of the 2.0 mL, 0.200 mL was used for CEMA content analysis spectrophotometrically at 274 nm. The rest was blown dry with nitrogen and then dissolved in 0.30 mL of THF for GPC analysis. GPC was performed with a Waters HT-4 column using THF as eluant.

Transmission Electron Microscopy. Solution samples were sprayed using a home-built device (Figure 1). Several drops of a solution were added into a tube containing a capillary open end and a male ground joint close to the other end.¹⁵ The tube was inserted into a socket with a female ground joint at one end. The length of the inserted tube was so adjusted that its capillary end just reached the narrow end of the socket. As the solution dripped out of the capillary, air, which was introduced from the sidearm of the socket and gushed out of the exit, broke the fine droplet from the inner tube and brought the particles into contact with a carbon-coated copper grid. Sprayed particles were stained with OsO₄ vapor overnight. For routine TEM experiments, a Hitachi-7000 transmission electron microscope (TEM) was operated at 100 kV. For observing a specimen at different TEM sample stage tilting angles, a Zeiss EM902 instrument was used.

Because of the large size, berrylike particles were sectioned for their internal structure examination by TEM. To ensure the integrity of the particles during TEM specimen preparation, a solution, in THF/AN with 80% AN 53 h after AN addition, was irradiated with UV light to achieve a PCEMA double-bond conversion of $\sim 30\%$.²³ The berrylike aggregates were then centrifuged out, dried, and embedded in an epoxy resin. The epoxy resin was cured at 60 °C for 1 day before the embedded sample was sectioned to 50 nm thick slices and stained with OsO₄ vapor overnight.

Light Scattering Measurements. Aggregates were prepared in the light scattering cells using filtered solvents for dynamic light scattering analysis. The solutions were not filtered or centrifuged before a measurement to avoid the removal of large particles. The measurements were conducted at a scattering angle of 90° using a Brookhaven model 9025 instrument equipped with an argon ion laser operated at 488 nm. The data were analyzed following the method of cumulants to obtain the hydrodynamic radius, R_h .¹⁶ The viscosities of THF/AN with 80%, 90%, and 93% AN determined using a Cannon Ubbelohde type viscometer are 0.356, 0.351, and 0.350 cP, respectively.

The change in the relative scattered intensity of a sample as a function of time was monitored using a fluorometer. In

this case, the excitation and emission wavelength were both set at 630 nm, and the excitation and emission slits were narrow to avoid signal saturation. The mixtures were prepared in a triangular cell so that the scattered intensity could be measured using the front-face mode.

III. Results and Discussion

Overall Pattern of Diblock Phase Segregation and Particle Growth. The water content in THF and AN had much influence on the phase segregation behavior of the diblock copolymer. When prepared using THF and AN directly taken out of bottles in the laboratory, the diblock copolymer was found to settle from THF/AN with 80%–93% AN within hours. Phenomena reported here are for mixtures prepared using THF and AN dried over molecular sieves overnight.

Immediately after the addition of AN dried over molecular sieves to a THF solution of the diblock, a mixture with a bluish tint appeared. Electron microscopic studies revealed the formation of spherical particles with PS core and PCEMA shell (Figures 2a and 3a). In THF/AN with 80% and 90% AN, the particle grew which was accompanied by morphological changes as illustrated in Figures 2a–d and 3a–d. While parts a–d of Figure 2 are TEM images obtained for the particles produced in THF/AN with 90% AN 5 min, 5, 23, and 53 h after AN addition, parts a–d of Figure 3 are particles prepared in THF/AN with 80% AN 20 min, 1, 23, and 53 h after AN addition. In THF/AN with 90% AN, the spherical particles evolved to egglike (Figure 2b) and then to onionlike and berrylike particles (Figure 2d). In THF/AN with 80% AN, egglike particles were never the dominant intermediate. The core–shell spherical particles seem to evolve directly into onionlike (Figure 3c) and then berrylike (Figure 3d) particles. In THF/AN with 93% AN the majority of the spherical particles did not mutate in 120 h as shown by electron microscopy.

The quick formation of spherical particles after AN addition and the subsequent particle morphological evolution were also confirmed by dynamic light scattering results. The diblock had a hydrodynamic radius, R_h , of 6.5 nm in THF, and the next R_h value we could measure soon enough after AN addition was ~ 25 nm. In THF/AN with 80% AN, the R_h values of the particles as illustrated in Figure 4 increased rapidly with time, suggesting the fast formation of large onionlike or berrylike particles, and leveled off ~ 40 h after AN addition. A gradual but moderate increase in R_h with time was seen for the particles prepared in THF/AN with 90% of AN, suggesting the slow formation of the relatively small egglike, onionlike, and berrylike particles. In THF/AN with 93% AN, the hydrodynamic radius, R_h , of the micelles increased slightly at times shorter than 0.5 h and then leveled off between 1 and 170 h.

Such quick formation of spherical particles after AN addition is also indirectly supported by data of Figure 5, where the intensity of scattered 630 nm light is shown to increase as a step function after AN addition. The scattered intensity from the THF/AN mixture with 80% AN increased over the whole observation period, but that from the mixture with 93% AN remained essentially constant after an initial jump. These are again in agreement with the dynamic light or TEM results that the morphology of the particles in THF/AN with 93% AN did not change over time but that in the mixture with 80% AN evolved with time.

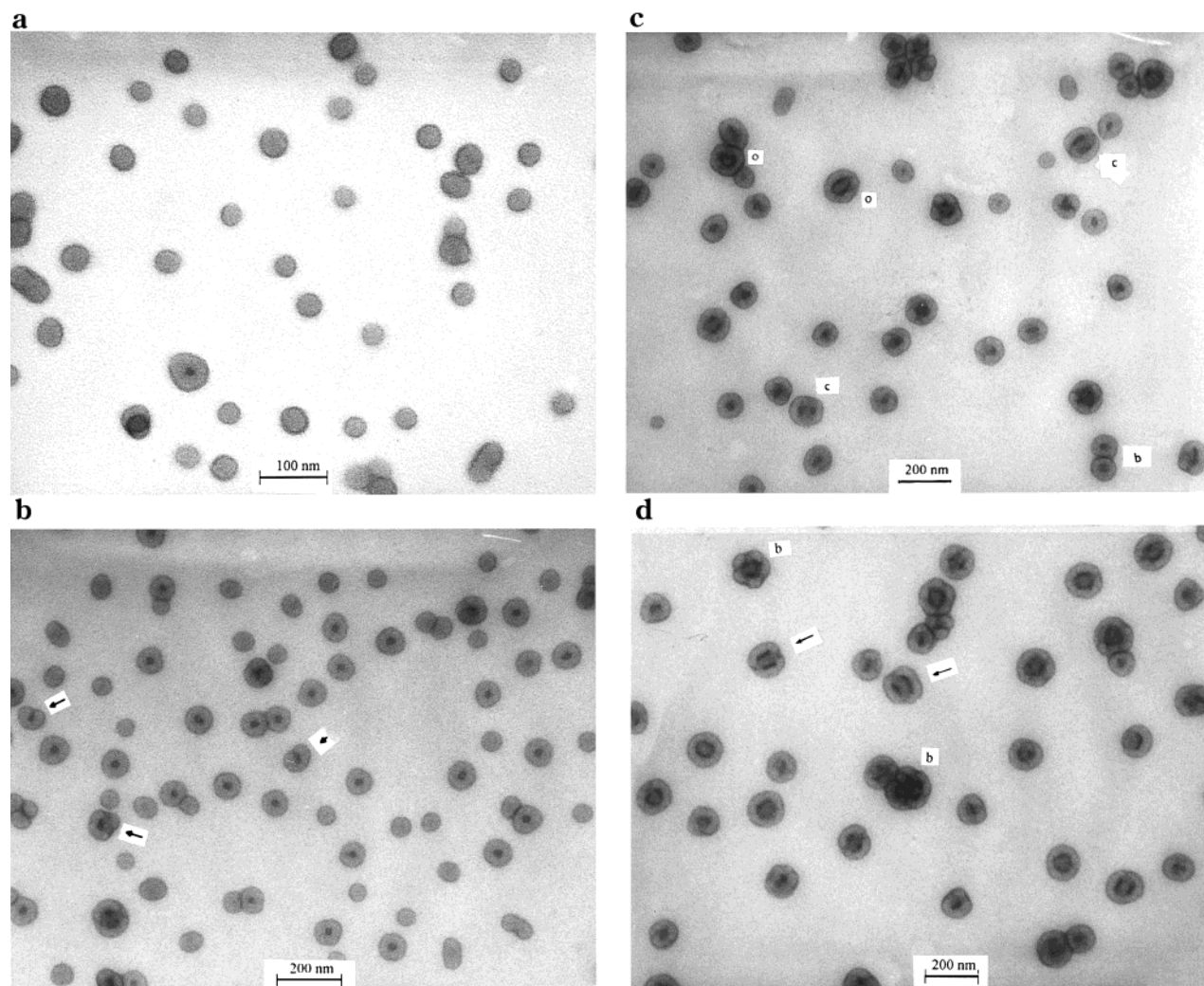


Figure 2. TEM images of PS-*b*-PCEMA micelles prepared in THF/AN with 90% AN 5 min (a, top left), 5 h (b, bottom left), 23 h (c, top right), and 53 h (d, bottom right) after AN addition. Indicated by arrows in (b) and (d) are some micelles in the process of being formed via the fusion of smaller micelles.

The quick formation of spherical particles suggests the swift phase separation of the diblock via either spinodal decomposition or nucleation. The particles eventually settled because they coalesced. In the subsequent sections, we will clarify the structural details of the particles formed before polymer precipitation.

Formation of Spherical Core–Shell Particles in the Initial Stage. Immediately after AN addition, spherical diblock particles with a diameter of ~ 20 nm formed as illustrated in Figures 2a and 3a. The particles are circular with dark periphery and gray interior. Since PCEMA contains double bonds and is more readily stained by OsO_4 , the aggregates must be spherical particles with PS core and PCEMA shell.

Our first assertion was that the spherical particles formed due to micelle formation. Although AN was a poor solvent for both PCEMA and PS, the THF/AN mixtures might dissolve the PCEMA block and make THF/AN block selective. To examine this possibility, we tested solubilities of a PS sample with a molar mass of 30 000 g/mol and two PCEMA samples with the molar masses of 9×10^5 and 9×10^3 g/mol in different THF/AN mixtures. Neither the PS nor the PCEMA sample with a higher molar mass dissolved in THF/AN with more than or equal to 80% AN. However, the lower molar mass PCEMA sample dissolved in THF/AN with less than or equal to 93% of AN. Thus, the PCEMA block

of our diblock with a molar mass of 5.5×10^4 g/mol might dissolve slightly in THF/AN mixtures used in this study.

The micelle formation interpretation was later ruled out, because micelles are thermodynamically stable species and should not precipitate out at long times. The more favored interpretation became particle formation due to polymer phase segregation.^{4,17}

The latter hypothesis was supported by several facts. First, the spherical particles of Figures 2a and 3a have a TEM radius, R_E , of ~ 25 nm. This size is typical for nuclei of a new phase.¹⁸ Second, the particles grew in size with time. This growth led to the eventual formation of egglike, onionlike, and berrylike particles. This growth was also reflected in the gradual size increase of spherical particles, as illustrated in Figures 2a,b and 4. The R_E value of the spherical particles sprayed from THF/AN with 90% AN 5 min after AN addition as revealed in Figure 2a is ~ 22 nm. This value jumped to ~ 33 nm 5 h after AN addition as shown in Figure 2b, a phenomenon which we never observed previously for micelles prepared in solvent/block-selective solvent mixtures. In THF/AN with 93% AN, the spherical morphology did not mutate in 120 h. The dynamic light scattering result of Figure 4 clearly indicated that the hydrodynamic radius jumped from 24.0 to 26.0 nm. Third, the spherical particles here are far denser than

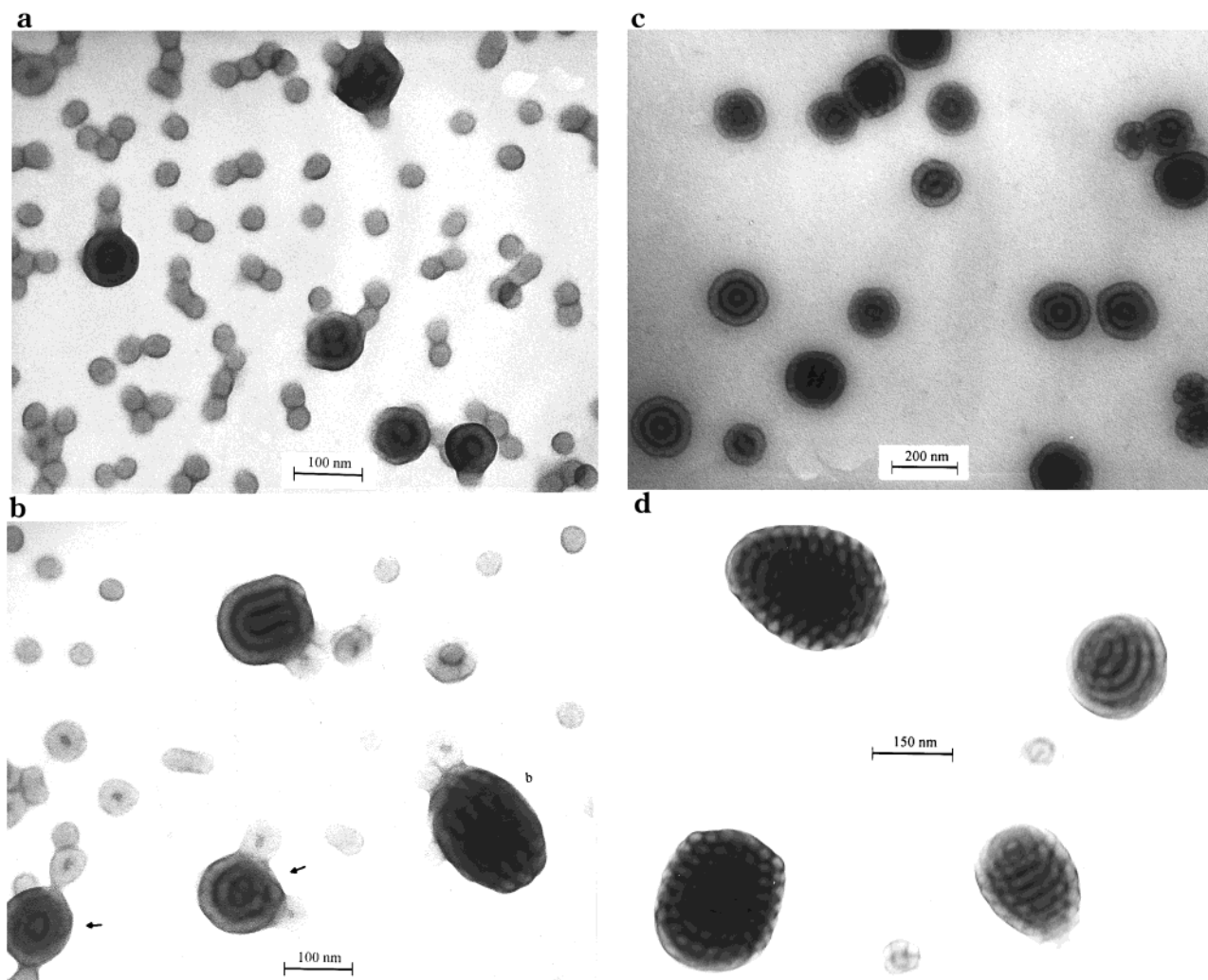


Figure 3. TEM images of PS-*b*-PCEMA micelles prepared in THF/AN with 80% AN 20 min (a, top left), 1 h (b, bottom left), 23 h (c, top right), and 53 h (d, bottom right) after AN addition.

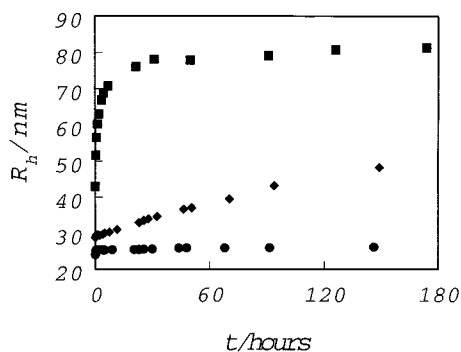


Figure 4. Variation in hydrodynamic radius, R_h , of the micelles as the function of time after AN addition. From bottom to top, the AN volume fraction decreases from 93% to 90% and 80%.

the micellar particles we studied previously. This is reflected in the comparable R_h and R_E values of the diblock particles, where R_h denotes the hydrodynamic radii determined by dynamic light scattering. The hydrodynamic radii, R_h , of the spherical micelles at short times prepared in THF/AN with 90% and 93% AN are ~ 29 and ~ 25 nm (Figure 4). These values agree well with the radii, R_E , of ~ 28 nm (the average radii of the spherical micelles 5 min and 5 h after their preparation)

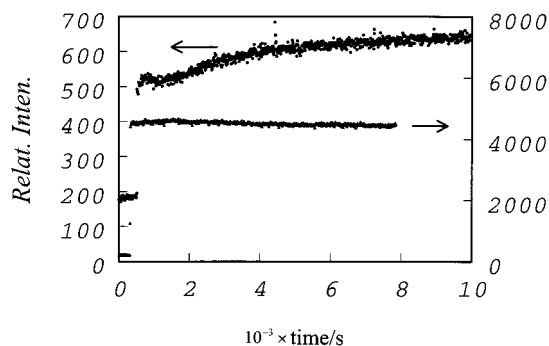


Figure 5. Variation in the relative scattered intensity as a function of time after AN addition for mixtures with the AN contents of 80% (●) and 93% (▲). The AN addition time is indicated by a sudden increase in the scattered intensity. The absolute intensities of the two samples are different, because the polymer concentrations used are different.

and ~ 23 nm determined from TEM. On the other hand, the R_h values of PS-*b*-PCEMA micelles in a block-selective solvent are significantly larger than R_E .¹⁹

Egglike Particles. As mentioned in the previous subsection, the R_E value of the spherical core-shell particles produced in THF/AN with 90% AN increased from ~ 22 to ~ 33 nm between 5 min and 5 h after AN addition. This growth in particle size with time is

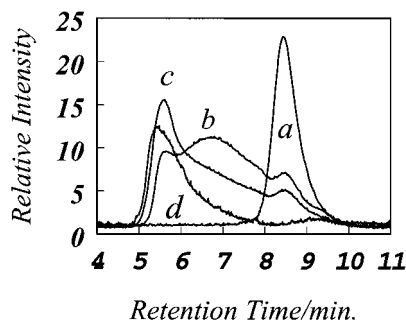


Figure 6. Evolution in the GPC chromatograms of egglike micelles irradiated in THF/AN with 90% AN as a function of CEMA conversion: (a) 0%, (b) 1.6%, (c) 11%, and (d) 29%.

probably due to the incorporation of more chains into existing particles by the nucleation and growth mechanism.^{1,2} For further particle growth in THF/AN with AN contents between 80% and 90%, particles with more complex morphologies, such as egglike particles of Figure 2b, were formed. This is understandable, because the chain lengths of the respective blocks limit the maximum size the simple core-shell particles can reach.

The egglike particles consist of a dark PCEMA core (resembling yolk of an egg), gray PS shell (white), and dark PCEMA outer shell (shell). Their TEM images resemble those of diblock vesicles formed in a block-selective solvent.^{8,20} They are definitely not vesicles, because a solvent pool should not exist in the center of such particles due to the poor quality of the THF/AN mixtures for either PS or PCEMA. The lack of a solvent reservoir in the center of the egglike particles can also be appreciated from the fact that the radius of the inner PCEMA domain is only ~12 nm, which is comparable to the unperturbed root-mean-square end-to-end distance of the PCEMA block with 210 CEMA units. Inside such a small inner PCEMA domain the PCEMA block should be able to distribute uniformly throughout.

Although the outer PCEMA shell should be quite compact due to the poor quality of the solvent mixtures for PCEMA, our experiment suggests that the outer PCEMA shell is, however, not as compact as the inner PCEMA domain, because chains of the inner PCEMA domain could be cross-linked more readily than the outer PCEMA chains. Compared in Figure 6 are the chromatograms of egglike particles formed in THF/AN with 90% AN 5 h after AN addition and irradiated to different CEMA conversions. Particles not irradiated were eluted out by THF as a single peak attributed to diblock chains. At the CEMA conversion of 1.6%, two higher molar mass peaks appeared. Further photolysis increased the intensity of the peak with the highest molar mass but decreased those of the peaks with lower molar masses. The observation of three peaks at a CEMA conversion of 1.6% is unique. We previously followed the GPC chromatogram change of spherical PS-*b*-PCEMA micelles with PCEMA cores¹⁴ and PS coronas¹⁹ as a function of irradiation dosage. In both cases, only two peaks were seen after sample photolysis with one peak attributed to unimer chains and the other to cross-linked or partially cross-linked micellar chains. The two higher molar mass peaks here must be from spherical particles with only their inner PCEMA domain cross-linked and those with both their inner and outer PCEMA domains cross-linked. As CEMA conversion increased, the population of the latter type of particles increased.

The more facile cross-linking of the inner PCEMA chains is also confirmed by TEM analysis of a sample with a CEMA conversion of 8%. When sprayed from THF, many spherical particles with a PCEMA radius of ~13 nm were observed by TEM. This radius is the same as that for the inner PCEMA domains of the egglike micelles in Figure 2b. A TEM image is not shown here for its poor contrast. The poor contrast is presumably caused by the presence of un-cross-linked or lightly cross-linked chains in the background.

Onionlike Particles. A further increase in the size of the particles led to the formation of onionlike particles. An onionlike particle has a light PS core and an outermost dark PCEMA shell with alternating dark PCEMA and light PS intermediate layers. Some onionlike particles are labeled with "o" in Figure 2c. A more spectacular view of onionlike particles is found in Figure 3c for particles in THF/AN with 80% AN 23 h after AN addition. Most of the onionlike particles in Figure 3c have four alternating dark and light intermediate layers. In THF/AN with 80% AN, the onionlike particles have an average radius of ~93 nm. The onionlike particles in Figure 2c,d have a radius of ~55 nm, which is significantly larger than the radius of ~43 nm for the egglike particles.

The spherical core-shell particles can be viewed as the simplest onionlike particles without intermediate layers between the PS core and PCEMA outermost shell. The egglike micelles are different from the onionlike particles in that the egglike particles have PCEMA instead of PS cores. The formation of egglike particles as the intermediate between the simple shell-core particles and onionlike particles was surprising. They formed probably due to the coalescence of different spherical particles and may invoke the following steps: (a) spherical particle encountering, (b) spherical particle local surface flattening to increase interparticle contact, (c) PCEMA chain receding to either the center or the surface of the fused particle, and (d) PS domains merging and egglike particle structure smoothing.

A rough idea about the 3-D structure of the onionlike particles was obtained by performing a TEM sample stage tilting experiment. A sample stage tilting instead of a shadowing experiment was performed for lack of facilities. Shown in Figure 7a,b are TEM images obtained of onionlike particles prepared in THF/AN with 80% AN 23 h after AN addition at the TEM sample stage tilting angles of 0 and 41°. The layered structure of the onionlike micelles did not change with the tilting angle variation. The fact that the image changed from circular to ellipsoidal suggests that the onions probably flattened somewhat on the TEM grid after sample spraying just like what was observed for the spherical and egglike particles.

The onionlike particles here have a similar morphology as the multilamellar vesicles or liposomes formed from small-molecule surfactants^{21–23} in water or from a polystyrene-*block*-polybutadiene, PS-*b*-PB, sample²⁴ in a PS homopolymer matrix (which functions as solvent). They are different because there are no solvent phases inside an onionlike particles. The lack of solvent pools inside the onionlike particles can be appreciated from the following considerations. First, the solvent mixtures are not good for either PS or PCEMA, and the creation of solvent pools and thus more interfaces between the polymer and solvents is not favorable. Then, the different PS and the inner PCEMA layers

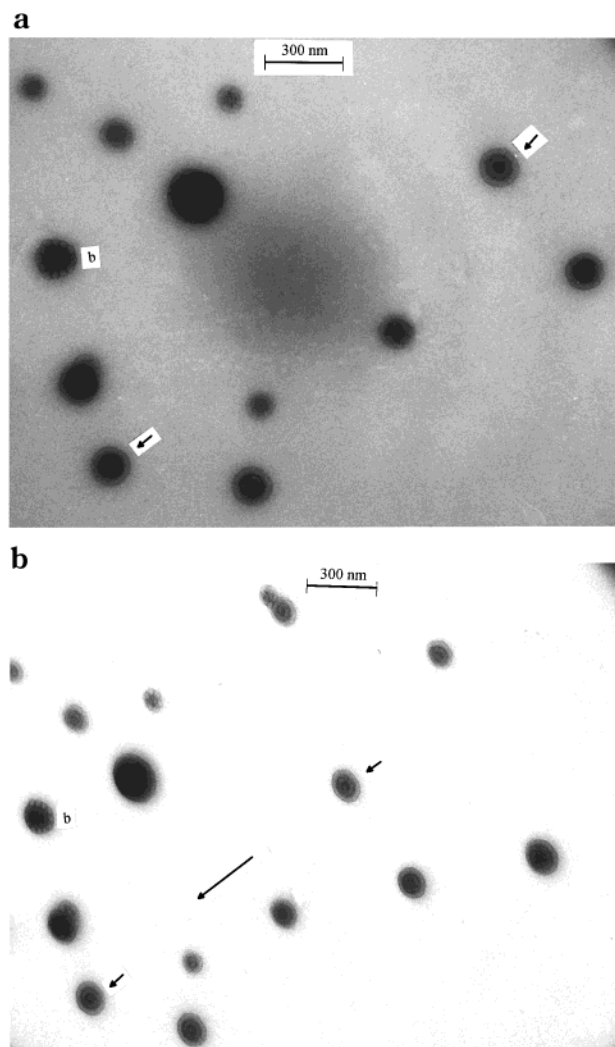


Figure 7. Comparison of TEM images of micelles prepared in THF/AN with 80% AN 23 h after AN addition at the sample stage tilting angles of 0 (top) and 41° (bottom). A berrylike micelle is marked with "b". The sample stage tilting direction is marked by a long arrow. Two short arrows are used to identify two onionlike micelles before and after the TEM sample stage rotation.

have high concentric symmetry. If the different layers are significantly swollen in solution, they would shrink nonuniformly along different directions and appear rugged upon drying as were seen previously for the shells of nanofibers²⁵ and star polymers.⁹ Third, the thicknesses of the PCMA and PS shells are only ~12 and ~20 nm in the onions of Figure 3c. Assuming that the average end-to-end distances, R_n , are approximately the same as the shell thickness and using the numbers, N , of C–C bonds of 420 and 760 for the PCMA and PS blocks, we calculated the statistical bond lengths, β , of 5.8 and 7.2 Å for PS and PCMA from

$$R_n = \sqrt{N}\beta \quad (1)$$

These β values are larger than the typical value of ~3.5–5.0 Å for unperturbed chains. It is difficult to imagine that the shells would swell much more in solution, because excessive chain stretching would increase the system's energy.

The name "onionlike particles" was from "onionlike micelles" used by Prochazka et al.²⁶ Onionlike micelles there are made of two diblock copolymers $(A)_l(B)_m$ and

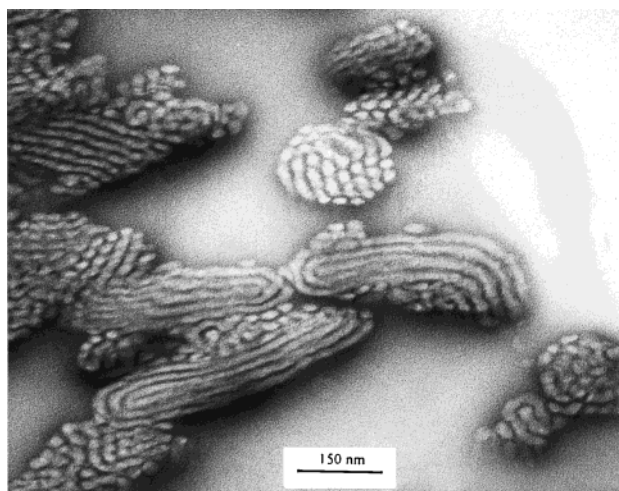


Figure 8. TEM image of a thin slice of berrylike micelles in THF/AN with 80% AN 53 h after AN addition.

$(B)_n(C)_k$ with a A–B–C three-layer structure and are structurally similar to those prepared from $(A)_n(B)_m(C)_l$ triblock copolymers.^{27–29} Our onionlike particles are structurally closer to those microdroplets prepared by Thomas et al. from a PS-*b*-PB sample.³⁰ The methodology used here is, however, different.

Berrylike Particles. Further growth of the particles in THF/AN with 80%–90% AN led to berrylike particle formation. Small "berries", labeled with "b", are seen in Figure 2d. Much larger berries are found in THF/AN with 80% AN (Figure 3d). The berrylike particles in THF/AN with 80% AN were found to be stable for a couple of weeks and then precipitated.

Of the large berries, only some small ones were imaged and shown in Figure 3d. The small berries were imaged to obtain contrast between different domains in the particles. A closer look at the internal structure of the particles was obtained by TEM studies of thin sections of the berrylike particles. Since the PCMA block was photo-cross-linked before the berries were embedded and sectioned, we do not expect significant morphological changes in the segregated PS and PCMA domains in a berry during TEM specimen preparation. Illustrated in Figure 8 is an image obtained of thin slices of the berrylike particles prepared in THF/AN with 80% AN 53 h after AN addition. In some particles, light stripes are separated by dark stripes. In others, hexagonally packed light circles are separated from one another by dark rings. These stripes and circles should correspond to hexagonally packed cylinders with PS core and PCMA shell lying parallel and perpendicular to the image planes. Some of the cylinders are seen to fold back on themselves at the boundary of a particle. The particles seem stabilized by a diffuse PCMA layer on the periphery.

This structural model is clearly in line with the images shown in Figure 3d. The berries shown on the left are those with the cylinders pointing out of the images. The cylinders in those on the right probably lie parallel to the image plane.

The images of the berrylike particles here resemble those observed by Zhang et al.^{31,32} for berrylike micelles formed from two other diblocks. They, however, differ in their internal structures. The berrylike micelles of Zhang et al. consisted of composite spheres²⁷ or hexagonally packed hollow loops.²⁸

Origin of the Aggregates. The concern with the solution spraying technique used by us is that the particles could have formed during specimen preparation. After nebulizing a dilute PS-*b*-PB solution (~0.1%) through a heated atmosphere to remove solvent, Thomas et al.,²⁸ for example, obtained polymer microdroplets with diameters between 10 and 50 nm, despite the fact that the polymer chains were initially well solvated and existed as isolated or slightly interpenetrating chains. The block-segregated PB and PS chains in the microdroplets had the same morphology as our PS-*b*-PCEMA onionlike particles.

Our particles could not have formed during specimen preparation, because particles with well-resolved PCEMA and PS domains were not seen after spraying the diblock from THF. The particles formed after spraying a THF solution had no definitive shape. The occasional spherical particles observed were not stable under the TEM electron beam.

We then proceeded to show that the morphology of the particles could not have mutated during specimen preparation. A given sample was divided into two portions with one portion being sprayed directly and the other being irradiated before spraying. The cross-linking of the PCEMA phase should "lock in" the particle structure, and such particles should not undergo significant structural mutation during solvent evaporation in the TEM specimen preparation step. The fact that the same morphology was always obtained for the same sample regardless of cross-linking suggests that the particle structures did not change significantly during TEM specimen preparation. In fact, the spraying method has been shown to retain the basic structural feature of block copolymer micelles in solution by many groups.^{20,33,34} This was established through the combined use of TEM, light scattering, NMR, FTIR, and our recent selective domain cross-linking or degradation experiments to vesicular^{15,35} and spherical micelles.³⁶ With structures very similar to those of diblock copolymer micelles of various geometries, our particles were expected to retain their basic features through the TEM specimen preparation process as well.

Other evidence supporting the formation of egglike, onionlike, or berrylike particles in solution includes the following. Only spherical or overlapping core-shell spherical particles (doublets) are seen in images taken of those prepared in THF/AN with 80% of AN 1 min after AN addition or of those prepared in THF/AN with 93% AN regardless of time span between AN addition and spraying (examined up to 120 h). If particle fusion during specimen preparation is the cause for the observation of the more complex particles, they should have appeared in these specimens as well. Particle fusion during TEM specimen preparation cannot explain the time evolution of the particle structures in THF/AN with 80% and 90% AN.

Variation in Particle Growth Rate with Solvent Composition. An examination of the phase diagram of a homopolymer-solvent-nonsolvent system reveals that increasing the nonsolvent content pushes the system more deeply into the metastable or the spinodal decomposition region,³⁷ and thus the polymer phase separation rate should increase. This may be true for our system but was not checked because phase separation occurred "instantaneously" or too fast for us to resolve with existing facilities even at the AN content of 80%. The dynamic light scattering results of Figure

4 clearly show that the rate of particle growth decreases with increasing AN content. As stated before, the growth of the diblock particles is also accompanied by morphological changes. The morphological change would require much position shuffling of the two blocks. An increase in the content of the precipitant and thus a decrease in the good solvent, THF, content may decrease particle swelling and lead to the locking of one of the blocks below its glass transition temperature. This locking in slows down morphological change and thus particle size growth.

The decrease in PS-*b*-PCEMA chain mobility with decreasing good solvent content has been previously demonstrated for micelles prepared in THF/cyclopentane (CP) mixtures, where CP solubilizes PS selectively.³⁸ For a diblock with 302 styrene and 37 CEMA units, the chain mobility decreased by 40-fold when the THF volume fraction decreased from 18% to 0% for THF/CP mixtures.

IV. Conclusion

Acetonitrile and THF are precipitants and good solvents for PCEMA and PS. THF/AN mixtures with AN volume fractions between 80% and 93% are precipitants for PS but slightly solubilize the PCEMA block of a PS-*b*-PCEMA sample with 210 CEMA units. In such solvent mixtures, spherical particles were formed from the diblock immediately after the addition of AN to a THF solution of the diblock due to phase separation. The spherical particles mutated into larger and more complex structures such as egglike, onionlike, and berrylike particles before polymer precipitation. The particle morphological mutation rate was found to decrease with increasing AN content, and in THF/AN with 93% AN, the structure of the spherical particles did not mutate in 1 week probably due to the locking in of the PS chains in a glassy state.

Acknowledgment. The Natural Sciences and Engineering Research Council of Canada is gratefully acknowledged for financially sponsoring this research. The authors also express deep gratitude to the reviewers for helping with the interpretation of the experimental observations. Royale Underhill is thanked for determining the hydrodynamic radius of the diblock in THF and for obtaining TEM images of the diblock sprayed from THF.

References and Notes

- (1) De Gennes, P. G. *Scaling Concepts in Polymer Physics*; Cornell University Press: Ithaca, NY, 1979.
- (2) See, for example: Gunton, J. D.; Miguel, M. S.; Sahni, P. S. In *Phase Transitions and Critical Phenomena*; Domb, C., Lebowitz, J. L., Eds.; Academic Press: New York, 1983; Vol. 8.
- (3) Krishnamurthy, S.; Bansil, R. *Phys. Rev. Lett.* **1983**, *50*, 2010.
- (4) Nakata, M.; Kawate, K. *Phys. Rev. Lett.* **1992**, *68*, 2176.
- (5) Sato, H.; Kuwahara, N.; Kubota, K. *Phys. Rev. E* **1994**, *50*, R1752.
- (6) Cumming, A.; Wiltzius, P. *Phys. Rev. Lett.* **1990**, *65*, 863.
- (7) Matsuura, T. *Synthetic Membranes and Membrane Separation Process*; CRC Press: Boca Raton, FL, 1993.
- (8) Ding, J.; Liu, G.; Yang, M. *Polymer* **1997**, *38*, 5497.
- (9) Tao, J.; Stewart, S.; Liu, G.; Yang, M. *Macromolecules* **1997**, *30*, 2738.
- (10) Ding, J.; Liu, G. *Macromolecules* **1997**, *30*, 655.
- (11) Liu, G. *Curr. Opin. Colloid Interface Sci.* **1998**, *3*, 200–208.
- (12) Liu, G.; Smith, C. K.; Hu, N.; Tao, J. *Macromolecules* **1996**, *29*, 220.
- (13) Tao, J.; Guo, A.; Liu, G. *Macromolecules* **1996**, *29*, 1618.
- (14) Guo, A.; Tao, J.; Liu, G. *Macromolecules* **1996**, *29*, 2487.

- (15) Ding, J.; Liu, G. *Chem. Mater.* **1998**, *10*, 537.
- (16) Koppel, D. E. *J. Chem. Phys.* **1972**, *57*, 4814.
- (17) See, for example: Krishnamurthy, S.; Goldburg, W. I. *Phys. Rev. A* **1980**, *22*, 2147.
- (18) Langer, J. S.; Schwartz, A. J. *Phys. Rev. A* **1980**, *21*, 948.
- (19) Ding, J.; Liu, G. *Macromolecules* **1998**, *31*, 6554.
- (20) Zhang, L.; Yu, K.; Eisenberg, A. *Science* **1996**, *272*, 1777.
- (21) Fendler, J. H. *Adv. Polym. Sci.* **1994**, *113*, 1.
- (22) Sharma, A.; Sharma, Ü. *Int. J. Pharm.* **1997**, *154*, 123.
- (23) Lasic, D. D. *Angew. Chem., Int. Ed. Engl.* **1994**, *33*, 1685.
- (24) Kinning, D. J.; Winey, K. I.; Thomas, E. L. *Macromolecules* **1988**, *21*, 3502.
- (25) Liu, G.; Qiao, L.; Guo, A. *Macromolecules* **1996**, *29*, 5508.
- (26) Prochazka, K.; Martin, T. J.; Webber, S. E.; Munk, P. *Macromolecules* **1996**, *29*, 6526.
- (27) Kriz, J.; Masar, B.; Plestil, J.; Tuzar, Z.; Pospisil, H.; Dorskilova, D. *Macromolecules* **1998**, *31*, 41.
- (28) Dormidontova, E. E.; Khokhlov, A. R. *Macromolecules* **1997**, *30*, 1980.
- (29) Stewart, S.; Liu, G. *Chem. Mater.* **1999**, *11*, 1048.
- (30) Thomas, E. L.; Reffner, J. R.; Bellare, J. *Colloq. Phys.* **1990**, *C7* (363), 15.
- (31) Zhang, L.; Yu, K.; Eisenberg, A. *Science* **1996**, *272*, 1777.
- (32) Zhang, L.; Bartels, C.; Yu, Y.; Shen, H.; Eisenberg, A. *Phys. Rev. Lett.* **1997**, *79*, 5034.
- (33) Price, P. *Pure Appl. Chem.* **1983**, *55*, 1563.
- (34) Thurmond II, K. B.; Kowalewski, T.; Wooley, K. L. *J. Am. Chem. Soc.* **1996**, *118*, 7239.
- (35) Ding, J.; Liu, G. *J. Phys. Chem. B* **1998**, *102*, 6107.
- (36) Tao, J.; Liu, G.; Ding, J.; Yang, M. *Macromolecules* **1997**, *30*, 4094.
- (37) De Witte, P. V.; Dijkstra, P. J.; Van den Berg, J. W. A.; Feijen, J. *J. Polym. Sci., Part B: Polym. Phys.* **1997**, *35*, 763.
- (38) Underhill, R. S.; Ding, J.; Birss, V. I.; Liu, G. *Macromolecules* **1997**, *30*, 8298.

MA990679V